Quaternary Geochronology 18 (2013) 78–92

Contents lists available at SciVerse ScienceDirect

Quaternary Geochronology

journal homepage: www.elsevier.com/locate/quageo

Research paper

Pleistocene magnetochronology of the fauna and Paleolithic sites in the Nihewan Basin: Significance for environmental and hominin evolution in North China

Hong Ao [a,*], Zhisheng An [a], Mark J. Dekkers [b], Yongxiang Li [c], Guoqiao Xiao [d], Hui Zhao [a], Xiaoke Qiang [a]

[a] State Key Laboratory of Loess and Quaternary Geology, Institute of Earth Environment, Chinese Academy of Sciences, Xi'an 710075, China
[b] Paleomagnetic Laboratory 'Fort Hoofddijk', Department of Earth Sciences, Faculty of Geosciences, Utrecht University, Budapestlaan 17, 3584 CD Utrecht, The Netherlands
[c] Institute of Cenozoic Geology and Environment, State Key Laboratory of Continental Dynamics, Department of Geology, Northwest University, Xi'an 710069, China
[d] State Key Laboratory of Biogeology and Environmental Geology, China University of Geosciences, Wuhan 430074, China

ARTICLE INFO

Article history:
Received 15 March 2013
Received in revised form
9 June 2013
Accepted 25 June 2013
Available online 4 July 2013

Keywords:
Magnetostratigraphy
Nihewan Fauna
Human evolution
Paleoenvironment
Nihewan Basin
Pleistocene

ABSTRACT

The fluvio-lacustrine sequences in the Nihewan Basin of North China (known as the Nihewan Formation) are rich sources of Early Pleistocene Paleolithic sites and mammalian fossils (known as the Nihewan Fauna sensu lato), which offer an excellent opportunity to investigate the evolution of early humans and land mammals in East Asia. Also abundant mammalian fossils provide clues about the general environmental and climatic setting of early humans. Among the Nihewan Fauna (sensu lato), the Daodi Fauna is one of the most complete and oldest in the eastern Nihewan Basin: seven mammalian fossil-bearing layers in the Nihewan Formation have been described. Except for a biostratigraphy, however, precise age control on the Daodi Fauna has remained unavailable. Here we report a new magnetostratigraphic record that stringently constrains its age. The seven fossil-rich layers span an age range of ca 2.5–1.8 Ma between the Gauss–Matuyama boundary and the termination of the Olduvai polarity subchron. Combining our new and recently published paleomagnetic data, we further establish a Pleistocene magnetochronology of the fauna and Paleolithic sites in the Nihewan Basin. Age ranges of about 2.5–0.5 Ma for the faunas and 1.7–0.3 Ma for the Paleolithic sites are deduced, which span most of the Pleistocene. The chronological framework and calculated proportions of mammals that were adapted to different environments indicate that mixed settings of dominant grasslands and subordinate forests continued at least from 2.5 to 0.5 Ma for early human occupation in the basin, similar to the mixed open savannah and woodland habitats of early humans in Africa. The Nihewan hominins consistently adopted a simple Oldowan-like technology (i.e., Mode 1 core and flake technologies) from at least ca 1.7 to 0.3 Ma. A more advanced Acheulean technology (Mode 2) has not been found in the Nihewan Basin, although it started to emerge in the Bose Basin of South China at ca 0.8 Ma. This implies that multiple groups of hominins distinguished by differential stone-tool-making capabilities may have coexisted in China after 0.8 Ma.

1. Introduction

The Nihewan Basin is an intermontane basin in North China (Fig. 1). It is well-known for its well-developed late Cenozoic fluvio-lacustrine strata that are rich in Early Pleistocene Paleolithic sites and mammalian faunas (Barbour, 1924; Teilhard de Chardin and Piveteau, 1930; Zhou et al., 1991; Xie, 2006; Xie et al., 2006; Zhu et al., 2007; Deng et al., 2008; Dennell, 2009; Keates, 2010; Yuan et al., 2011; Ao et al., 2013). The fluvio-lacustrine sequence, which has been named the Nihewan Formation (or Beds) (Barbour, 1924; Deng et al., 2008; Ao et al., 2013), is the type section of the Early Pleistocene in North China (Young, 1950). These fauna sites are known as the Nihewan Fauna (sensu lato). The abundant Lower Paleolithic sites and Pleistocene faunas in the Nihewan Formation

* Corresponding author. Tel.: +86 29 88321470.
E-mail addresses: aohong@ieecas.cn, ah_wjf@yahoo.com.cn (H. Ao).

1871-1014
http://dx.doi.org/10.1016/j.quageo.2013.06.004

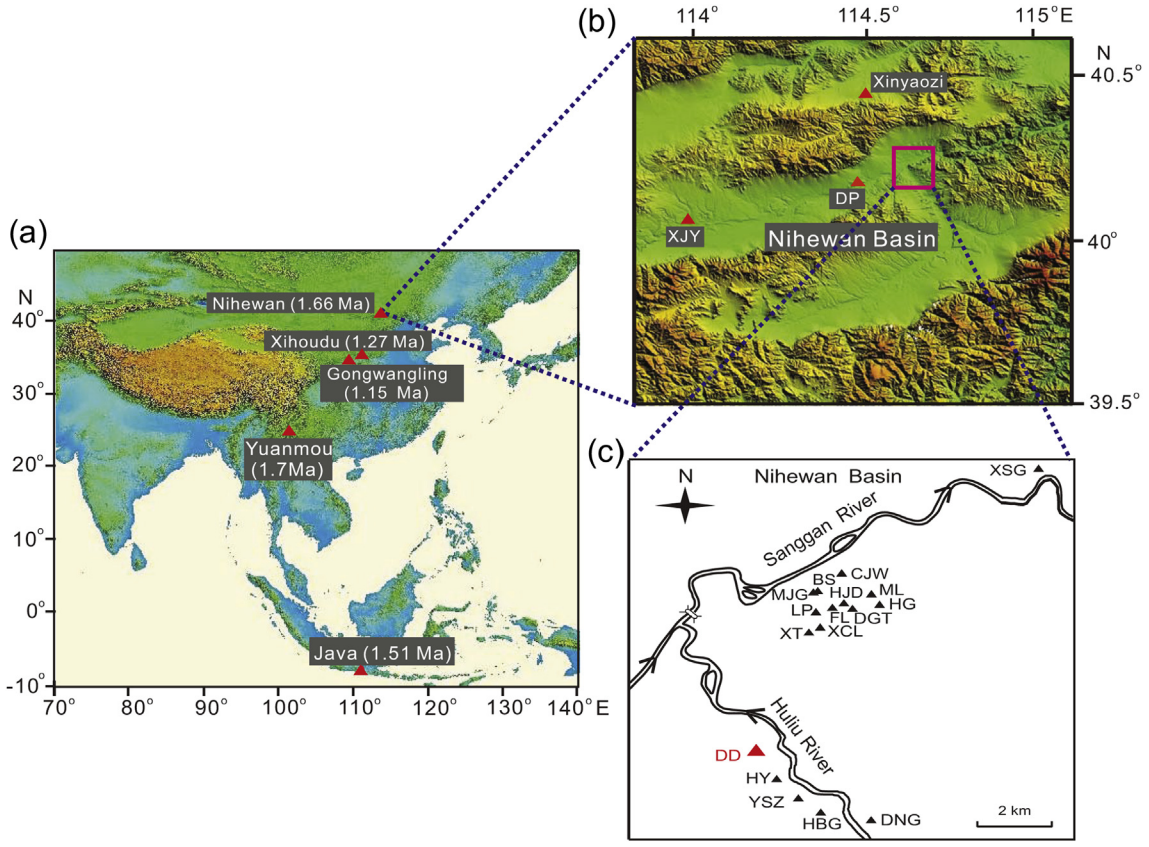

Fig. 1. Schematic map of the Nihewan Basin and the Paleolithic and fauna sites mentioned in this paper. XJY, Xujiayao; DP, Dongpo; DNG, Danangou; HBG, Huabaogou; YSZ, Yangshuizhan; HY, Hongya; DD, Daodi; XT, Xiantai; XCL, Xiaochangliang; LP, Lanpo; FL, Feiliang; HJD, Huojiadi; DGT, Donggutuo; HG, Hougou; ML, Maliang; MJG, Majuangou; BS, Banshan, CJW, Chenjiawan; XSG, Xiashagou.

make the basin ideal for investigating early human and mammal evolution in North China.

The Early Pleistocene or Late Pliocene faunas in the Nihewan Basin (e.g., Teilhard de Chardin and Piveteau, 1930; Qiu, 2000; Zhang et al., 2003; Li et al., 2008) are crucial for providing environmental information associated with early human evolution in North China (Dennell, 2009). Paleontological studies have indicated that the Nihewan Fauna possibly contains not only Pleistocene but also Late Pliocene faunas (Wang, 1982; Zhou et al., 1991; Zhang et al., 2003; Li et al., 2008). In particular, the earliest Hongya (HY), Huabaogou (HBG) and Daodi (DD; also named Laowogou) faunas in the eastern Nihewan Basin were suggested to extend possibly to the Late Pliocene (Wang, 1982; Zhang et al., 2003; Li et al., 2008). Since 2009, the Pleistocene–Pliocene boundary has been redefined at an age of 2.58 Ma instead of the previous allocation at ~1.8 Ma (Gibbard and Head, 2010). Accordingly, the magnetostratigraphic age estimates of ca 2.4 Ma for the HY Fauna and 1.9–1.7 Ma for the HBG Fauna (Deng et al., 2008) now fall within the Early Pleistocene. In order to date the previously undated DD Fauna and to test whether it occurred during the Early Pleistocene like the HBG and HY faunas, we carried out a detailed magnetostratigraphic investigation on the DD section. This work places stringent age controls on its mammalian fossil-bearing layers. Combining the present study and recently published paleomagnetic data, we further establish a combined Pleistocene magnetochronology of the fauna and Paleolithic sites in the Nihewan Basin, which serves as a basis for further discussion of implications for early human evolution in North China.

2. Study site

Our investigated DD section (40°9′N, 114°39.5′E) is located on the western bank of the Huliu River, less than 2 km north of the HY section (Fig. 1). The ca 128 m of horizontal Nihewan Formation outcrop is capped by Late Quaternary surface soils (~1 m). As is the case for the nearby Yangshuizhang (YSZ) (Ao et al., 2013), HY and HBG sections (Deng et al., 2008) (Fig. 1), the Nihewan Formation of the DD section can be divided into two parts: an upper part consisting of grayish-green and grayish-yellow silty clays and clayey silts intercalated with conglomerate or sand layers, and a lower part comprising lacustrine red silty clay. In the DD section, the stratigraphic boundary between the two parts is located at a depth of ~99 m (whereby the top is defined as 0 m). Generally, the conglomerates in the upper part are reasonably well sorted, with few angular and sharp pebbles and cobbles. The three thick conglomerate layers located at ca 2, 18 and 28 m have erosive bases, which are possibly indicative of sedimentary hiatuses. In addition, seven layers that contain mammalian fossils have been found; the fossil mammals of each layer are listed in Table 1 (finds from Cai, 1987; Zhang et al., 2003; Cai et al., 2004; Li et al., 2008). The fossil list is dominated by micromammals; large mammals are mainly found in the DD-4 layer. A large number of genera and species of the DD Fauna were shown to be similar to other Middle to Late Pliocene faunas in North China (Zhang et al., 2003; Li et al., 2008). For example, the presence of *Chardinomys yusheensis*, *Chardina truncates*, *Micromys tedfordi* and *Huaxiamys downsi* in the DD-1 layer (Table 1) makes it correlatable with the Leijiahe Fauna from

Table 1
List of the mammal fossils of the DD section at different layers (finds from Cai, 1987; Zhang et al., 2003; Cai et al., 2004; Li et al., 2008).

Taxa	DD-1 2.54 Ma	DD-2 2.34 Ma	DD-3 2.02 Ma	DD-4 1.92 Ma	DD-5 1.9 Ma	DD-6 1.84 Ma	DD-7 1.78 Ma
Allocricetus bursae							+
Antilospira sp.				+			
Apodemus cf. A. agrarius		+					
Apodemus cf. A. atavus					+		
Apodemus sp.		+	+				
Apodemus zhangwagouensis	+	+			+		
Axis shansius				+			
Castor anderssoni					+		
Cervus sp.				+			
Chardina truncatus	+						
Chardinomys nihowanicus	+	+		+	+		+
Chardinomys yusheensis	+	+	+				
Chilotherium sp.				+			
Dipus fraudator				+	+		
Germanomys cf. G. weileri			+				
Germanomys sp.		+	+				
Huaxiamys downsi	+						
Huaxiamys primitivus	+						
?Huaxiamys sp.	+						
Karnimata sp.				+	+		
Kowalskia similis	+						
Kowalskia sp.	+						
Lunanosorex cf.*L.lii*					+		
Mesosiphneus praetingi				+	+		
Micromys tedfordi	+	+	+	+			
Mimomys orientalis			+	+	+		
Mimomys sp.		+	+	+	+		
Mimomys sp. 2				+			
Mimomys stenlini		+					
Nannocricetus mongolicus	+	+	+	+	+		+
Ochotona minor					+		
Ochotona sp.		+	+			+	
Paenelimnoecus chinensis				+			
Paralactaga andersoni			+	+			
Pliosiphneus sp.		+	+				
Pliosiphneus sp. 2		+					
Proboscidipparion sinense				+	+		
Pseudomeriones complicidens		+	+				
Quyania sp.					+		
Saidomys sp.				+	+		
Sinocricetus procressus	+	+		+	+		
Sinocricetus zdanskyi			+	+	+		
Sminthoides fraudator				+	+		
Sorex sp.		+				+	+
Trimylus sp.				+			
Trischizolagus sp.	+						
Ungaromys spp.	+	+			+		

Lingtai county, Gansu province (Northwestern China) (Li et al., 2008). The presence of *C. yusheensis*, *Chardinomys nihowanicus*, *M. tedfordi*, *Apodemus zhangwagouensis* and *Mimomys* in the DD-2 layer (Table 1) makes it correlatable with the Mazegou Fauna from the Yushe Basin, Shanxi province (North China) (Li et al., 2008). The Lingtai county and Yushe Basin are about 900 and 400 km southwestern of the Nihewan Basin, respectively. Both the Leijiahe and Mazegou faunas were considered as Middle to Late Pliocene faunas in North China (Flynn et al., 1997; Zheng and Zhang, 2001), thus the DD Fauna was thought to extend to the Late Pliocene according to the previous allocation of Pleistocene–Pliocene boundary at ~1.8 Ma (Zhang et al., 2003; Li et al., 2008).

3. Sampling and measuring methods

In order to obtain samples that were as fresh as possible, at least 30 cm of the outcrop was removed to eliminate potential weathering effects and disturbance due to vegetation. A total of 344 block samples were oriented by magnetic compass in the field and were taken at 30–40 cm stratigraphic intervals. From each block sample, two cubic specimens of 2 cm × 2 cm × 2 cm were subsequently cut in the laboratory for thermal demagnetization treatment. Some unheated left-overs of these block samples were used for rock magnetic analyses. All rock magnetic and paleomagnetic measurements were performed at the Institute of Earth Environment, Chinese Academy of Sciences (IEECAS, Xi'an, China).

Before thermal demagnetization, the anisotropy of magnetic susceptibility (AMS) was measured for all 344 levels (i.e., 1 sample for each level) using a MFK1-FA Kappabridge (Agico Ltd., Brno). Furthermore, six samples from different magnetozones were selected for both temperature-dependent susceptibility (χ–T) and isothermal remanent magnetization (IRM) acquisition measurements. All χ–T curves were measured in an argon atmosphere at a frequency of 976 Hz from room temperature up to 700 °C and back to room temperature using a MFK1-FA Kappabridge instrument equipped with a CS-3 high-temperature furnace (AGICO, Brno, Czech Republic). The magnetic field during measurement was 300 A/m (peak-to-peak). In order to determine the temperature-dependent background χ, a run with an empty furnace tube

was performed before measuring the sediment samples. The susceptibility of each sediment sample was obtained by subtracting the measured background χ (furnace tube correction) using the CUREVAL 5.0 program (AGICO, Brno, Czech Republic). IRM acquisition curves were determined using an ASC IM-10-30 pulse magnetizer up to a maximum field of 2.7 T and an AGICO JR-6A spinner magnetometer for remanence measurements. IRM acquisition curves consist of 34–37 IRM field steps.

Stepwise thermal demagnetization was conducted using a TD-48 thermal demagnetizer. Most samples were stepwise heated at 10–50 °C temperature increments to a maximum temperature of 680 °C or occasionally to 640 °C when >90% of the initial remanence was demagnetized, which was usually associated with unstable oscillation of the measured paleomagnetic directions. After each demagnetization step, remanence was measured using a 2-G Enterprises Model 755-R cryogenic magnetometer housed in a magnetically shielded space. The demagnetization results were evaluated using orthogonal vector component diagrams (Zijderveld, 1967). The principal component direction was computed for each sample using a least-squares fitting technique (Kirschvink, 1980). The principal component analyses were conducted using the PaleoMag software developed by Jones (2002).

4. Results

4.1. Rock magnetism

For the 344 levels from the DD section, the magnetic fabric is generally oblate, with the magnetic foliation (*F*) larger than the magnetic lineation (*L*) (Fig. 2a). The minimum susceptibility axes (K_{min}) of the AMS ellipsoid are mainly close to the vertical, perpendicular to the bedding plane; so the maximum axes (K_{max}) are close to the horizontal, parallel to the bedding plane (Fig. 2b). This AMS behavior is consistent with a primary sedimentary fabric (e.g., Rees and Wooddall, 1975; Wang et al., 2005; Liu et al., 2010a).

Six χ–*T* curves from the DD section are shown in Fig. 3. Consistent with the ubiquitous occurrence of magnetite, all the heating curves are characterized by a major drop near 585 °C. Each sample also undergoes a steady χ increase below 300 °C during heating, which may result from the gradual unblocking of fine-grained (i.e., superparamagnetic (SP) and small single-domain (SD)) ferrimagnetic particles or the release of stress upon heating (van Velzen and Zijderveld, 1995; Liu et al., 2005, 2010b; Deng et al., 2006a). A χ drop between 300 and 500 °C in some heating curves is interpreted as being due to the conversion of ferrimagnetic maghemite to weakly magnetic hematite (Løvlie et al., 2001; Deng et al., 2006b, 2008) or to changes in crystallinity, grain size or morphology of the magnetic particles during heating (Dunlop and Özdemir, 1997; Ao, 2008; Ao et al., 2009). The χ of hematite is about two orders of magnitude lower than that of magnetite. Its presence is usually masked magnetically by the much stronger contribution of magnetite, thus its behavior on the χ–*T* curves is generally poorly expressed when both minerals are present. Hematite also occurs in the Nihewan fluvio-lacustrine sediments as suggested by IRM acquisition curves (Fig. 4), progressive thermal demagnetization analyses (Fig. 5), and other studies (Løvlie et al., 2001; Wang et al., 2004, 2005; Deng et al., 2006b; Ao et al., 2010a). In addition, each sample has an increased χ during cooling after heating to 700 °C (Fig. 3), which may result from the neo-formation of fine-grained magnetite via annealing of a mixture of hematite and iron-containing paramagnetic silicates/clays (e.g., chlorite) (Tanikawa et al., 2008; Ao et al., 2009; Zhang et al., 2010, 2012).

Consistent with the dominant contribution of magnetite to the magnetic mineralogy, all IRM acquisition curves undergo a major increase below 300 mT (Fig. 4). However, these curves are generally not saturated at 1 T and increase slightly between 300 and 2700 mT (Fig. 4), which provides evidence for the presence of high-coercivity hematite.

4.2. Paleomagnetism

In most samples from the DD section, the natural remanent magnetization (NRM) is composed of two components: (1) a secondary low-temperature component (LTC) isolated by progressive demagnetization to 150–250 °C (occasionally up to 400 °C) followed by (2) a characteristic remanent magnetization (ChRM) component isolated at higher temperatures (Fig. 5). After removal of the secondary LTC magnetization, the ChRM shows a relatively straightforward unidirectional trajectory toward the origin in the orthogonal plots. For most samples, the ChRM component was identified up to 680 °C, while thermal demagnetization up to 640 °C is also sufficient to isolate the ChRM component for a few samples. This behavior indicates that (possibly partially oxidized) magnetite and hematite are the main carriers of the ChRM (Deng et al., 2006b, 2007; Liu et al., 2010a, 2012). Reliable ChRM directions are established based on (1) at least four (but typically 8–16) consecutive demagnetization steps starting at least at 250 °C, (2) a maximum angular deviation (MAD) ≤15° and (3) a calculated virtual geomagnetic pole (VGP) latitude >30° or <−30° (May and Butler, 1986; Zhu et al., 2008; Ao et al., 2013). Among the

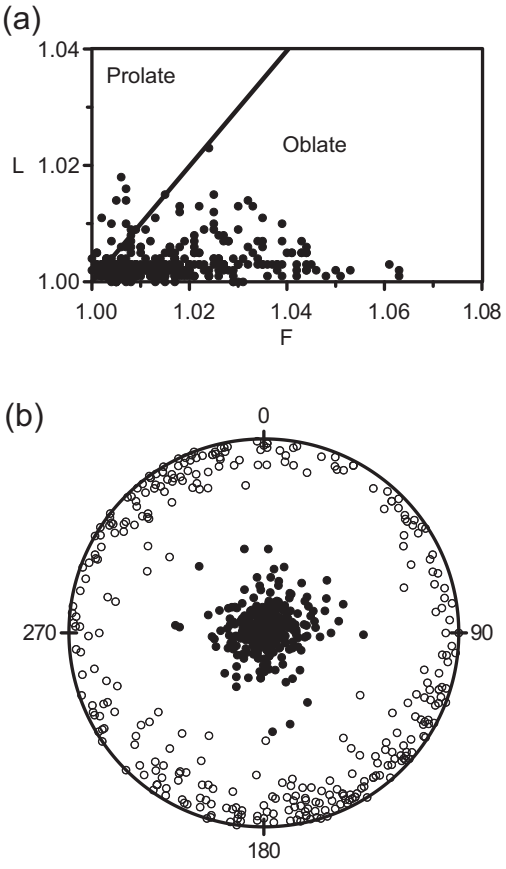

Fig. 2. Anisotropy of magnetic susceptibility (AMS) of samples from the DD section. (a) Magnetic lineation (*L*) versus magnetic foliation (*F*), (b) Stereographic projection (bedding coordinates) of principal susceptibility axes of K_{max} (open squares) and K_{min} (solid circles).

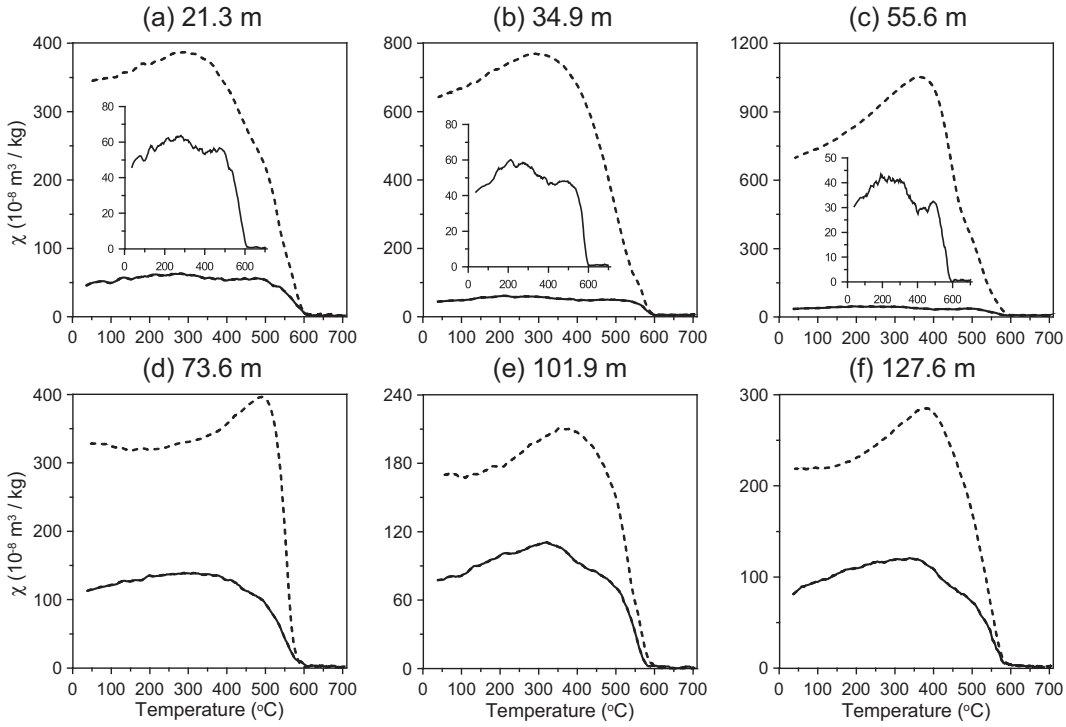

Fig. 3. χ–T curves for selected samples from the DD section. Solid (dashed) lines represent heating (cooling) curves.

344 measured levels, 214 (62%) meet these criteria. These ChRM directions result in an antipodal distribution of 107 normal and 107 reversed orientations on the equal area projection (Fig. 6a). The normal ChRM directions yield an overall mean of declination $D = 357.8^\circ$ and inclination $I = 51.7^\circ$ ($\kappa = 18.6$, $\alpha_{95} = 3.3^\circ$; κ is the precision parameter and α_{95} is the radius of the 95% confidence cone around the mean direction). The reversed ChRM directions yield an overall mean of $D = 183.9^\circ$ and $I = -49.7^\circ$ ($\kappa = 12.9$, $\alpha_{95} = 4.0^\circ$). Furthermore, the reversal test (McFadden and McElhinny, 1990; Tauxe, 1998) is positive (Fig. 6b) with an angular difference of 4.3° between the overall mean directions of each polarity. This is less than the 95% radius of confidence angle of

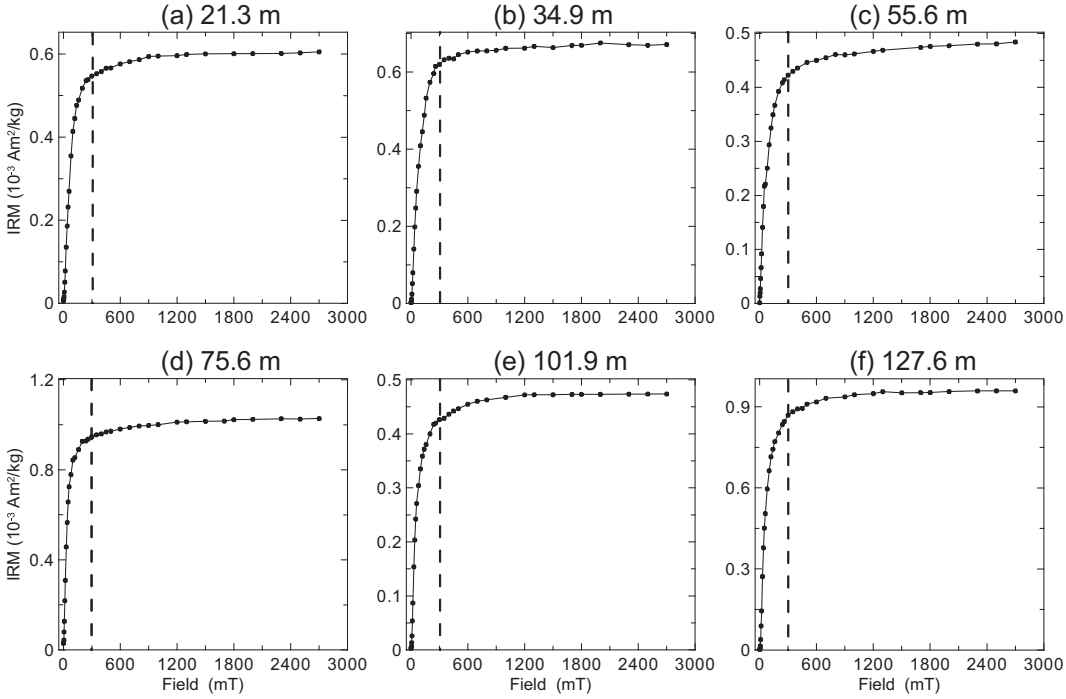

Fig. 4. Isothermal Remanent Magnetization (IRM) acquisition curves for selected samples from the DD section. The dashed vertical lines at 300 mT are shown to aid distinction between low- and high-coercivity portions of the IRM acquisition curves.

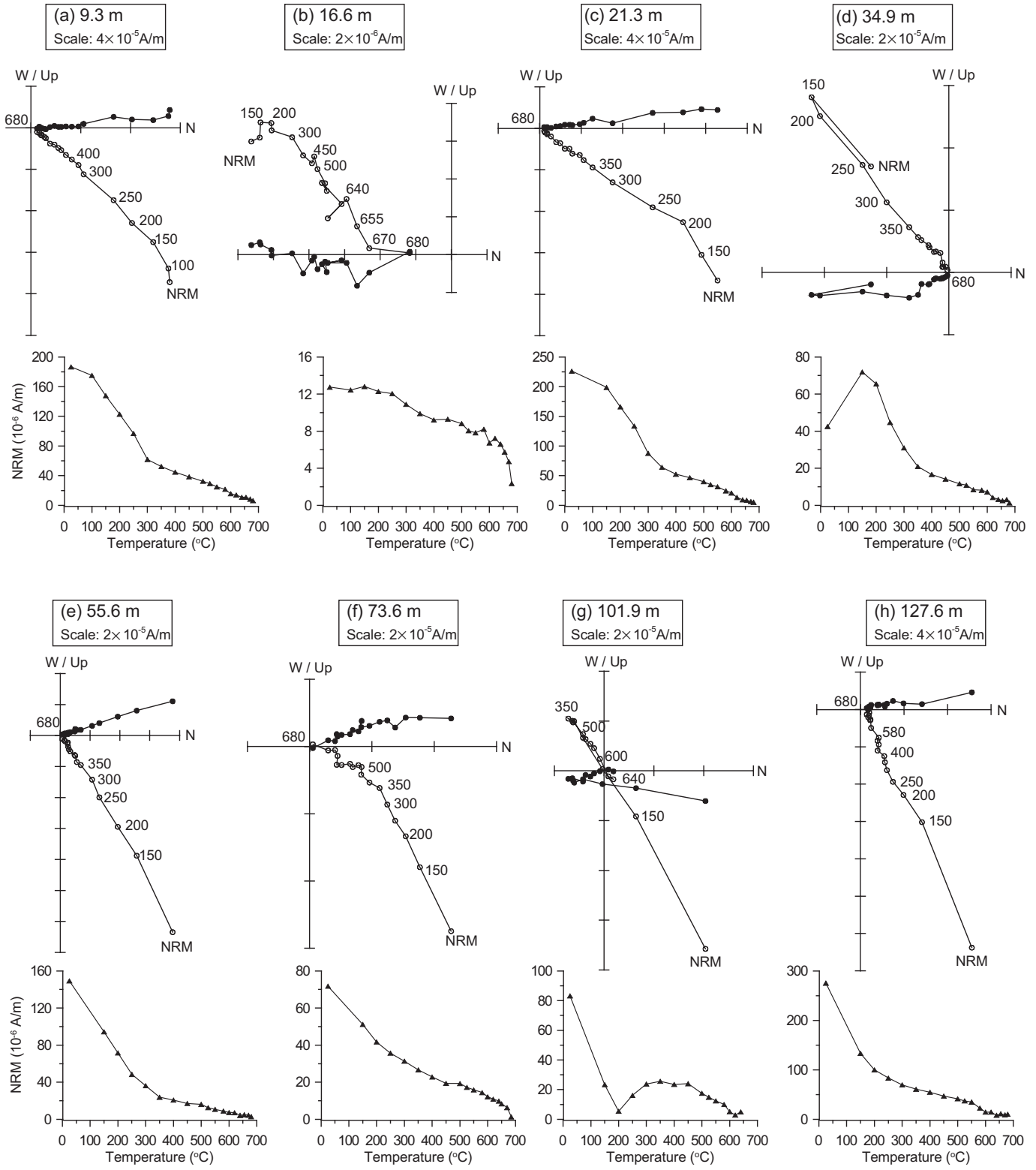

Fig. 5. The direction and intensity evolution of the NRM during stepwise thermal demagnetization for selected samples from the DD section. Open and closed symbols in the orthogonal vector endpoint projections (Zijderveld, 1967) indicate projections on to the vertical and horizontal planes, respectively. The numbers refer to the demagnetization temperatures in °C. NRM is the natural remanent magnetization.

5.1° and yields a class B reversal test (McFadden and McElhinny, 1990). Finally, the virtual geomagnetic pole (VGP) latitudes calculated from all the 214 ChRM directions are used to define the magnetostratigraphic polarity column of the DD section (see Fig. 7 and Table A. 1). Seven main polarity intervals are identified: four normal and three reversed. Generally, the polarity column has no correlation with the NRM variability that was usually of the order of 10^{-3}–10^{-6} A/m. The four normal magnetozones are not characterized by unusual NRM values. This implies that they are less likely to involve in remagnetization.

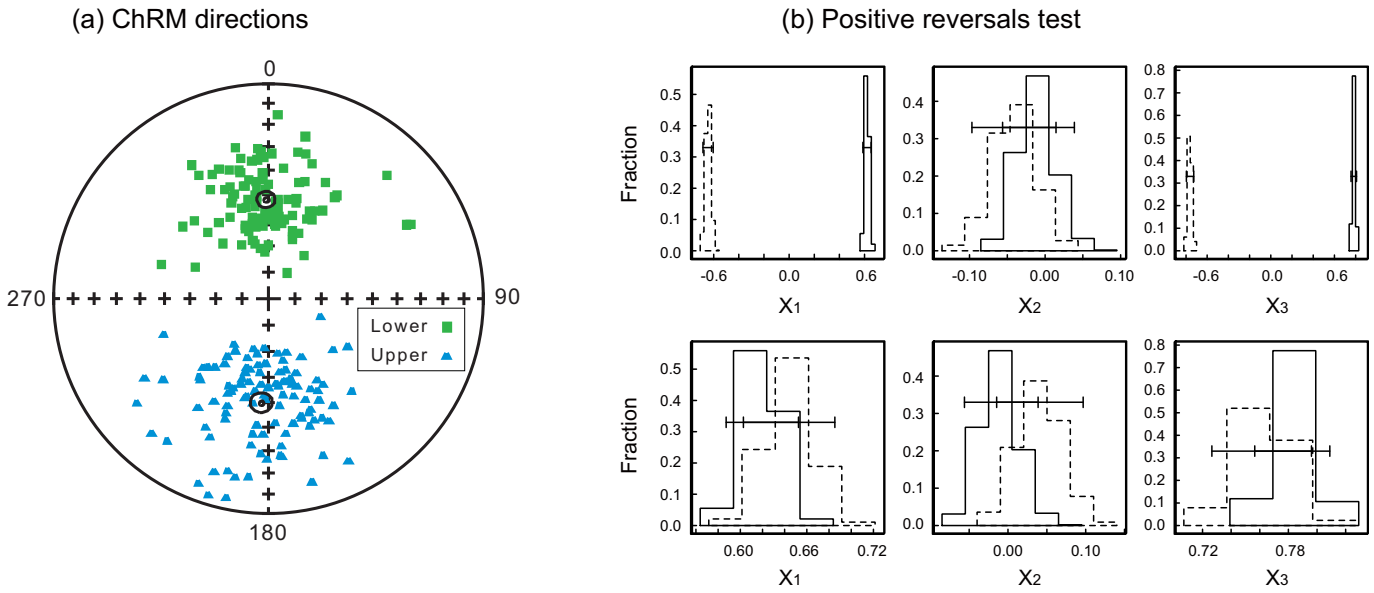

Fig. 6. (a) An equal area projection of 214 directions of the high-temperature ChRM component of the DD section samples. The green squares and blue triangles represent the downward and upward ChRM directions, respectively. (b) Bootstrap reversal test diagram (Tauxe, 1998) of ChRM. Reversed polarity directions have been inverted to their antipodes to test for a common mean for the normal and reversed magnetization directions. The means of the normal and reversed modes cannot be distinguished at the 95% level of confidence, indicating a positive bootstrap reversal test. (For interpretation of the references to colour in this figure legend, the reader is referred to the web version of this article.)

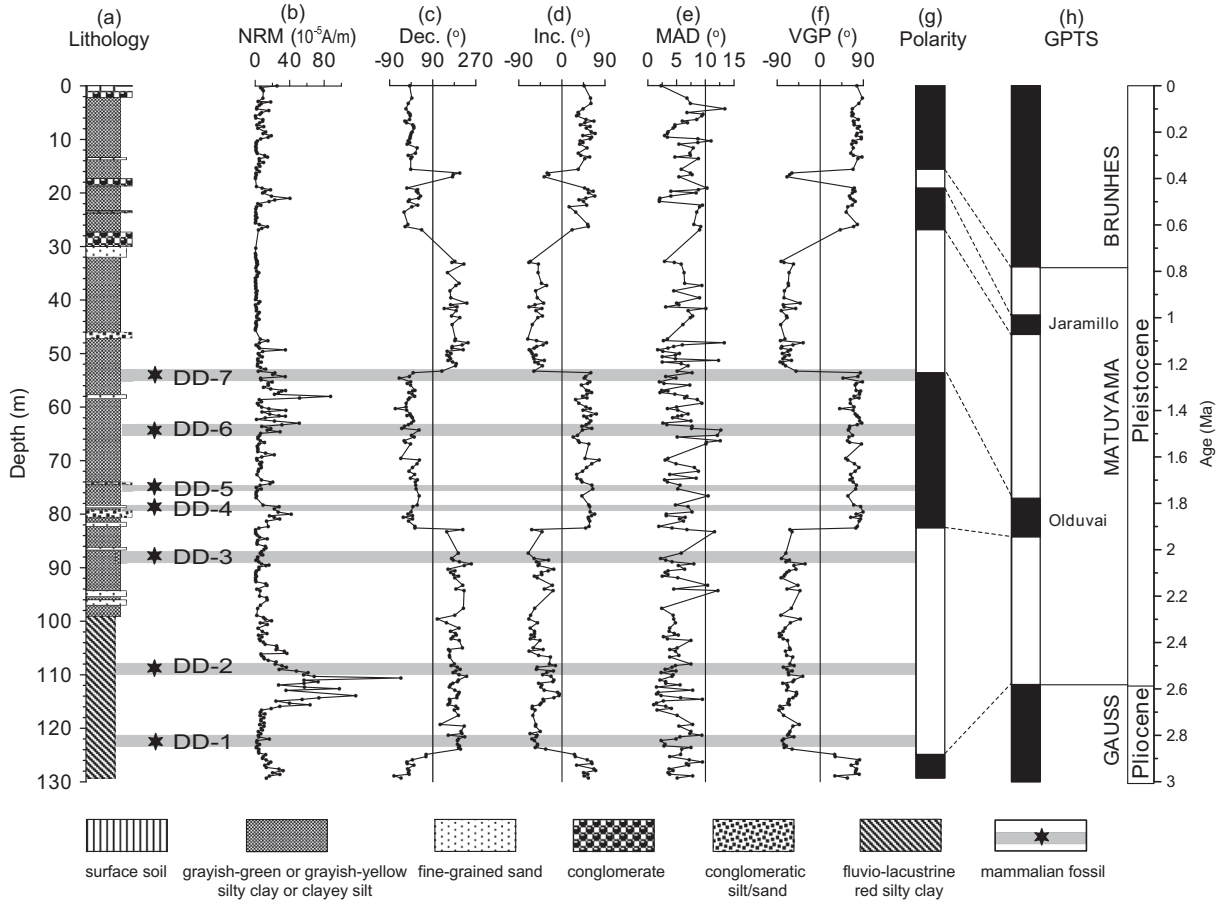

Fig. 7. Lithostratigraphy and magnetostratigraphy of the DD section and correlation with the geomagnetic polarity timescale (GPTS). (a) Lithology, (b) natural remanent magnetization (NRM), (c) declination (Dec.), (d) inclination (Inc.), (e) maximum angular deviation (MAD), (f) virtual geomagnetic pole (VGP) latitude, and (g) paleomagnetic polarity sequence of the DD section. (h) Geomagnetic polarity timescale (GPTS) (Hilgen et al., 2012).

5. Discussion

5.1. Magnetostratigraphy and age estimation of the Daodi Fauna

Based on the recent magnetostratigraphy of the Nihewan Formation in nearby sections (Fig. 8) and the biostratigraphy and sedimentology of the DD section, the most plausible correlation of the magnetostratigraphic polarity sequence determined for the DD section to the Geomagnetic Polarity Time Scale (GPTS) (Hilgen et al., 2012) is shown in Fig. 7. The correlation suggests that at the DD section the Nihewan Formation records a geomagnetic polarity pattern that spans from the late Gauss normal polarity chron to the lowermost Brunhes normal polarity chron. The Gauss–Matuyama geomagnetic reversal boundary, which corresponds approximately to the Pliocene–Pleistocene boundary (Gibbard and Head, 2010), is located at 124.9 m. The Matuyama–Brunhes boundary is located at a depth of 15.6 m. The Jaramillo (19.1–26.9 m) and Olduvai (53.6–82.6 m) normal polarity subchrons were identified in the Matuyama reversed chron.

Our new magnetostratigraphy of the DD section is comparable to the recently established magnetostratigraphic records from the nearby YSZ (Ao et al., 2013), HY and HBG sections (Deng et al., 2008), which are all located on the western bank of the Huliu River (see Fig. 1 for locations), with similar variability of lithology (Fig. 8). The DD and YSZ sections both have a relatively shortened reversed polarity magnetozone between the top of the Jaramillo polarity subchron and the bottom of the Brunhes polarity chron, which could imply the presence of a sedimentary hiatus or decreased sedimentation rates within this interval. Based on the occurrence of a ca 1.5-m thick conglomerate layer within this interval, the former interpretation may be more likely for the DD section. All four studied sections have a relatively shortened reversed polarity magnetozone between the bottom of the Jaramillo polarity subchron and the top of the Olduvai polarity subchron. The presence of conglomerate layers in this interval could imply sedimentary hiatuses within this stratigraphic interval (Fig. 8). These lines of evidence thus indicate significant changes in averaged sedimentation rates for the Nihewan Formation, which vary over different periods and at different sections (Fig. 9). Except for the HBG section, the other three sections (i.e., HY, DD and YSZ) are all characterized by high sedimentation rates during the Olduvai polarity subchron. This implies a strong riverine input during that period and/or that the depocenter of the

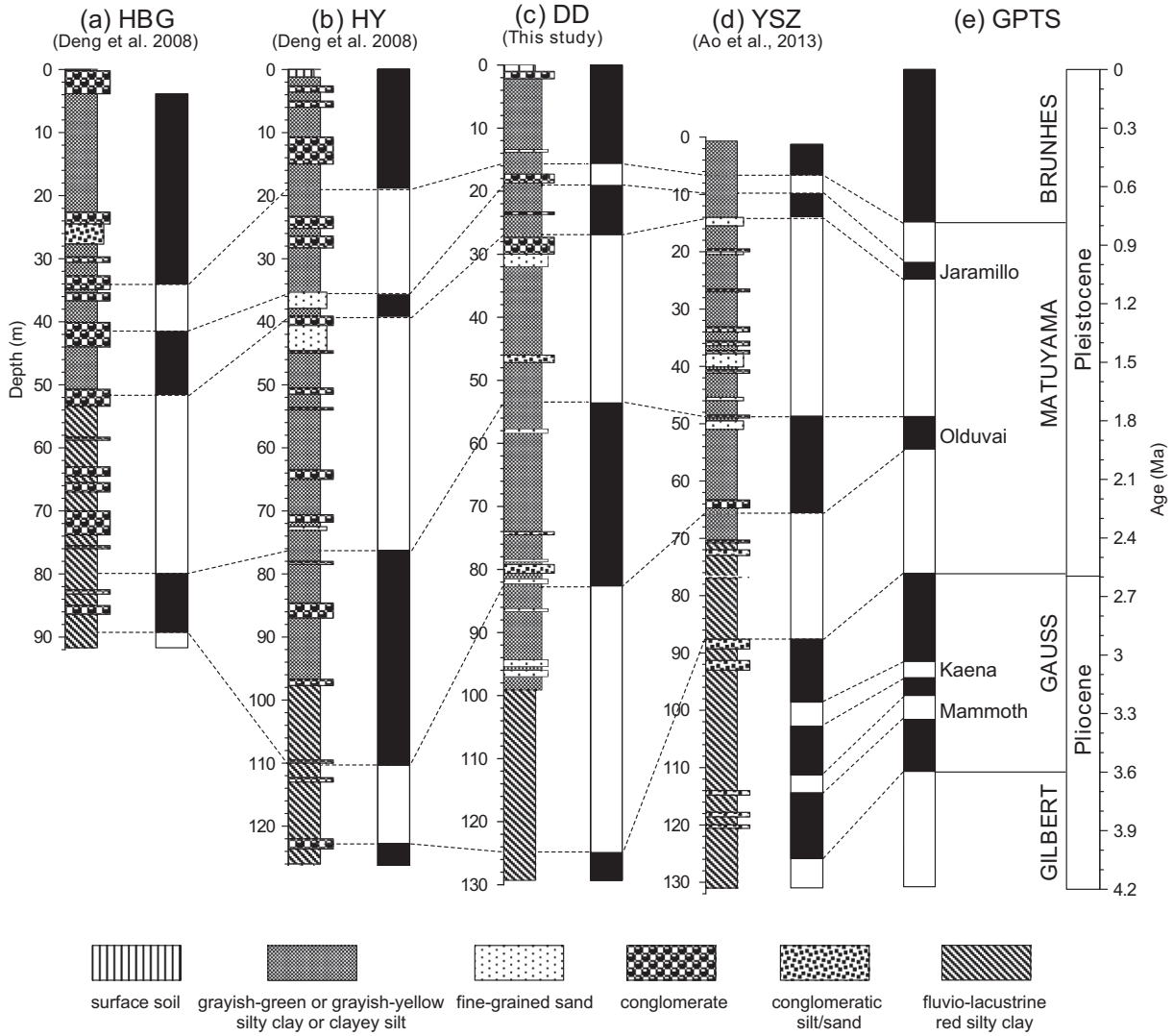

Fig. 8. Comparison of magnetostratigraphic records from several typical sections in the eastern Nihewan Basin and their correlation to the geomagnetic polarity timescale (GPTS). Lithostratigraphy and magnetostratigraphy from sections: (a) HBG (Deng et al., 2008), (b) HY (Deng et al., 2008), (c) DD (this study), (d) YSZ (Ao et al., 2013) (see Fig. 1 for locations). (e) GPTS (Hilgen et al., 2012).

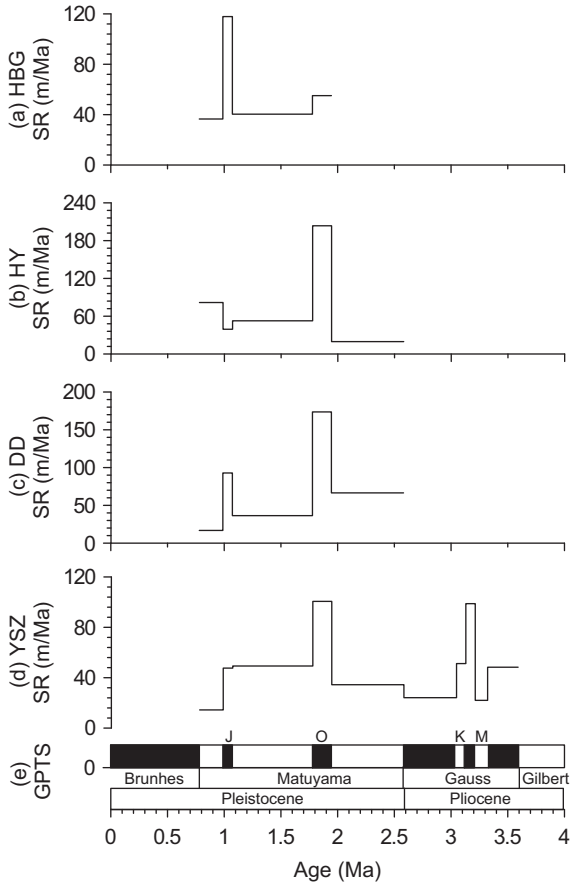

Fig. 9. Sedimentation rate (SR) variability of (a) HBG, (b) HY, (c) DD and (d) YSZ sections. (e) GPTS (Hilgen et al., 2012). J, Jaramillo; O, Olduvai; K, Kaena; M, Mammoth.

Nihewan paleolake possibly occurred in this area. We should bear in mind, however, that the consistent presence of prolonged Olduvai polarity subchron in the three nearby sections provides additional evidence for their reliable magnetostratigraphic correlation. Relatively high sedimentation rates within the Jaramillo polarity subchron are also observed in the HBG and DD sections (Fig. 9). In addition, the YSZ section shows a high sedimentation rate between the lower boundary of Kaena and upper boundary of Mammoth (Fig. 9). These marked variations of sedimentation rates is common in the continental fluvio-lacustrine strata of the eastern Nihewan Basin (Deng et al., 2008; Ao et al., 2013). It is generally interpreted as due to local synsedimentary faulting, major changes of sedimentary environments in different periods, different paleotopography, distance to the paleoshore, or riverine input to these sections (Deng et al., 2008; Ao et al., 2013).

Based on our magnetostratigraphy, we estimate the average ages of the layers rich in mammalian fossils within the DD section (Fig. 7). The DD-1 (~122 m), DD-2 (~109 m) and DD-3 (~88 m) mammal-bearing layers are located between the Gauss–Matuyama boundary and the lower boundary of Olduvai polarity subchron. Linear interpolation of sedimentation rates in this interval indicates an age of ~2.54 Ma for DD-1, ~2.34 Ma for DD-2 and ~2.02 Ma for DD-3, respectively. The DD-4 (~79 m), DD-5 (~75 m) and DD-6 (~64 m) mammal-bearing layers are located in the Olduvai polarity subchron. Linear interpolation of sedimentation rate in this interval indicates an age of ~1.92 Ma for DD-4, ~1.9 Ma for DD-5, and ~1.84 Ma for DD-6, respectively. The youngest fossil-bearing layer DD-7 (~54 m) is located at the upper boundary of the Olduvai polarity subchron, yielding an estimated age of ca 1.78 Ma. Therefore, the DD Fauna appears to be located between the Gauss–Matuyama boundary and termination of the Olduvai polarity subchron, ranging in time from ca 2.5 to 1.8 Ma (Fig. 7). Like the HBG and HY faunas (Deng et al., 2008), it fails to extend back to the "new" Late Pliocene.

5.2. Pleistocene magnetochronology of the Nihewan Fauna

We can now establish a magnetochronological framework for the faunas in the Nihewan Basin (Fig. 10a, b). Except for the Xujiayao (XJY) Fauna in the western basin (Fig. 1), which is dated to the middle Brunhes chron (Løvlie et al., 2001), all other mammalian faunas in the northeastern basin are located within the Matuyama chron. The DD-1 layer (ca 2.5 Ma) preserves the currently oldest Nihewan Fauna (sensu lato), but it is only slightly older than the HY Fauna (ca 2.4 Ma) (Deng et al., 2008). Another old fauna is the Xiashagou (XSG) Fauna (2.2–1.7 Ma), which ranges from the pre-Réunion period to after the Olduvai polarity subchron (Liu et al., 2012). The HBG-II Fauna is located within the lower Olduvai polarity subchron, with an estimated age of ca 1.9 Ma (Deng et al., 2008). The YSZ-II Fauna is located at the termination of the Olduvai polarity subchron, having an estimated age of ca 1.8 Ma (Ao et al., 2013). The HBG-I, Majuangou-III (MJG-III) and YSZ-I faunas occur later than the termination of the Olduvai polarity subchron, with an estimated age of ca 1.7 (Deng et al., 2008), 1.66 (Zhu et al., 2004) and 1.6 Ma (Ao et al., 2013), respectively. The Xiaochangliang (XCL) and Banshan (BS) faunas are relatively younger: they occur approximately halfway between the Olduvai and Jaramillo polarity subchrons, with an estimated age of ca 1.36 (Zhu et al., 2001) and 1.32 Ma (Zhu et al., 2004), respectively. The Donggutuo (DGT) and Maliang (ML) faunas are located just below the lower boundary of the Jaramillo polarity subchron and Matuyama–Brunhes boundary, yielding an estimated age of ca 1.1 and 0.8 Ma, respectively (Wang et al., 2005). The XJY Fauna is the currently youngest Nihewan Fauna, which has a magnetostratigraphic age of ca 0.5 Ma (Løvlie et al., 2001; Wang et al., 2008). Therefore, our established magnetochronological framework indicates that the Nihewan Fauna ranges from ca 2.5 to 0.5 Ma, spanning most of the Pleistocene. The time interval of 2.2–1.6 Ma appears to yield the most flourishing faunas (Fig. 10).

Our magnetostratigraphy of the Nihewan Fauna (Fig. 10) also refines the ages of some specific faunal elements of particular biochronological significance. For example, the occurrence of *Coelodonta antiquitatis* in the XSG Fauna (2.2–1.7 Ma) (Table 2) indicates that the *Coelodonta* (woolly rhino), a mammal adapted to cold climate and steppe conditions, migrated into the Nihewan Basin from the Tibetan Plateau during the Early Pleistocene soon after the intensification of Northern Hemisphere glaciation (Deng et al., 2011). *Equus przewalskii*, another steppe mammal that is highly adapted to dry and cold climates, started to appear in the XJY Fauna (Table 2) after the Mid-Pleistocene when more severe glaciations occurred as inferred from increased amplitudes of climate variability (Lisiecki and Raymo, 2005) (Fig. 10g).

There are also several other typical Early Pleistocene mammalian faunas, such as the Danangou (Li, 1984), Dongyaozhitou (Tang, 1980; Zhou et al., 1991) and Xinyaozi (Zhou et al., 1991) faunas (Table 3) in the northeastern Nihewan Basin, which are not yet well-dated using magnetostratigraphy. However, comparison of the faunal elements with other well-dated faunas indicates that all the three faunas are younger than the HBG Fauna (<1.9 Ma) (Zhou et al., 1991; Deng et al., 2008).

Following the formation of the Nihewan paleolake since the Mid-Pliocene (Ao et al., 2013), the Nihewan Basin attracted many large mammals including species from other continents (e.g., Africa and America) before 2 Ma (Fig. 10 and Tables 1–3). For example,

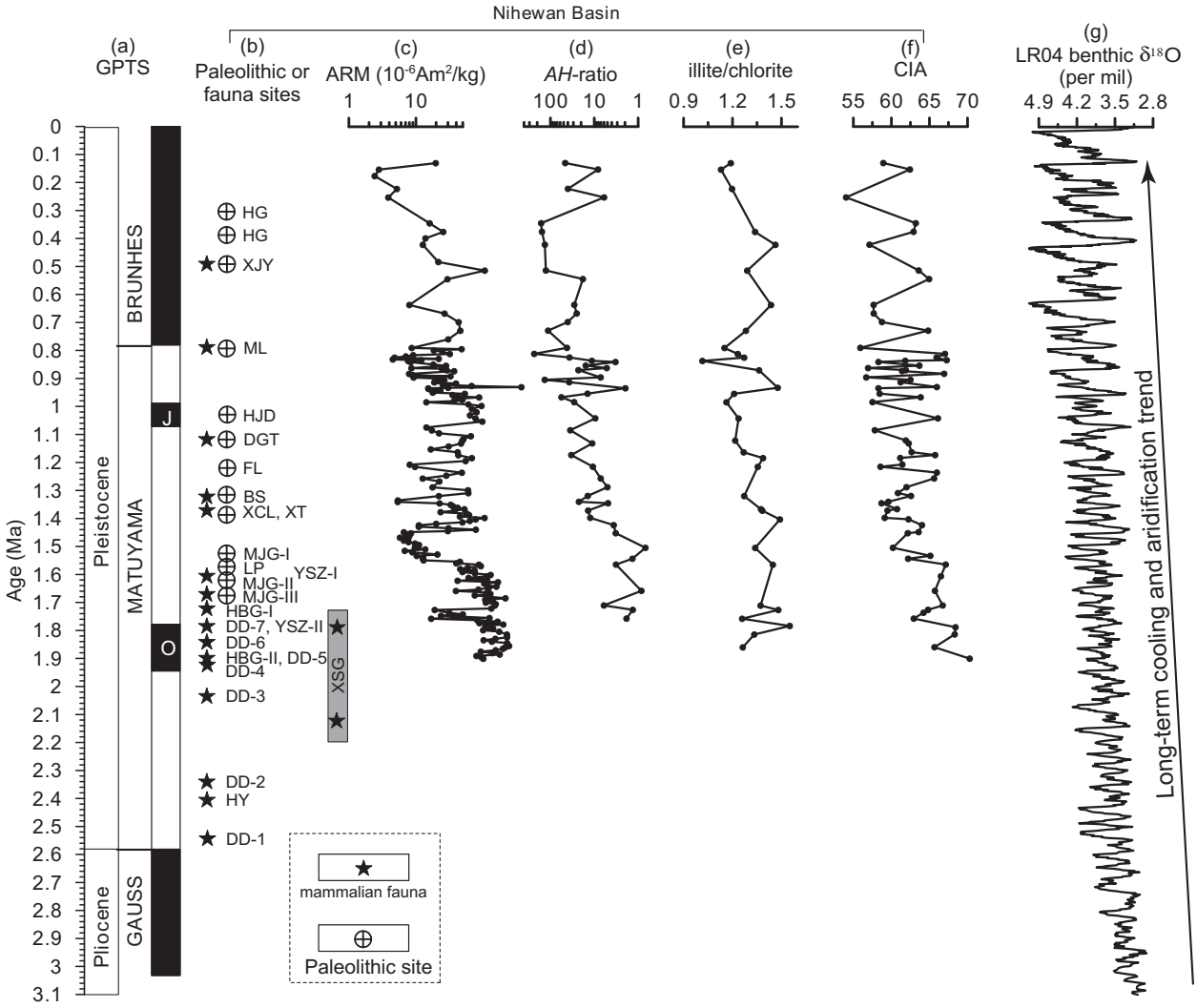

Fig. 10. Synthesis of all magnetostratigraphically dated fauna and Paleolithic sites in the Nihewan Basin within the framework of the geomagnetic polarity timescale (GPTS) and temporal variability of regional and global climate during the Quaternary. (a) GPTS (Hilgen et al., 2012). J, Jaramillo; O, Olduvai. (b) Well-dated fauna and Paleolithic sites in the Nihewan Basin using magnetostratigraphy. Data sources for ages: HG (Zuo et al., 2011), XJY (Løvlie et al., 2001; Wang et al., 2008), ML (Wang et al., 2005), HJD (Liu et al., 2010a), DGT (Wang et al., 2005), FL (Deng et al., 2008), BS (Zhu et al., 2004), XCL (Zhu et al., 2001), XT (Deng et al., 2006b), LP (Ao et al., 2012), MJG (Zhu et al., 2004), HBG (Deng et al., 2008), DD (this study), XSG (Liu et al., 2012), HY (Deng et al., 2008), YSZ (Ao et al., 2013). Magnetoclimatological proxies: (c) anhysteretic remanent magnetization (ARM) (Ao, 2010) and (d) *AH*-ratio (Ao et al., 2009) (*AH*-ratio characterizes the relative amount of newly formed fine-grained ferrimagnetic minerals during heating, which is linked to the relative concentration of chlorite in the samples. For a more detailed description see the cited reference), (e) illite/chlorite ratio (Ao et al., 2009) and (f) chemical index of alteration (CIA) (Ao et al., 2010b) from the Nihewan Formation at the Xiantai section. (g) LR04 benthic δ^{18}O stack (Lisiecki and Raymo, 2005).

Palaeoloxodon antiques (straight tusked elephant), which originated in Africa (Beden, 1980), has also been found in the XSG Fauna (2.2–1.7 Ma) (Liu et al., 2012) (Table 2). Consistent with the dispersal of Proboscideas out of Africa during the 2.5–1.5 Ma time interval (Tchernov and Shoshani, 1996), *Hipparion* sp. was also found in the HY Fauna (2.4 Ma) (Deng et al., 2008). In addition, the occurrence of *Equus sanmeniensis* in the XSG Fauna indicates that *Equus* migrated from North America to the Nihewan Basin via the Bering Strait soon after 2.6 Ma when the intensification of major Northern Hemisphere glaciations made the sea retreating from the Bering Strait (Lindsay et al., 1980; Deng and Xue, 1999; Wang and Deng, 2011).

5.3. Environmental significance of the Nihewan Fauna

Long-term high-resolution environmental records directly retrieved from the Nihewan Formation are rare. Up to now, only a few long-term environmental records are available. For example, the anhysteretic remanent magnetization (ARM) record from the XT section (Fig. 10c) indicates a long-term decreasing trend in magnetic mineral concentration linked to a long-term decrease in abundance of magnetic minerals in the catchments and in transportation of detrital magnetic minerals into the Nihewan paleolake (Ao, 2010). This is attributed to a long-term decrease in East Asian monsoon precipitation in the Nihewan Basin during the Pleistocene (Ao, 2010). A long-term decrease in chemical weathering intensity in the Nihewan Basin during the Pleistocene is also suggested by the magnetoclimatological proxy termed *AH*-ratio, clay mineralogical proxy illite/chlorite and chemical index of alteration (CIA) (Ao et al., 2009, 2010b) (Fig. 10d–f). The *AH*-ratio characterizes the relative amount of newly formed fine-grained ferromagnetic minerals during heating, which is linked to the relative concentration of chlorite in the samples (for a more detailed description see Ao et al. (2009)).

Table 2
List of mammal faunas in the Nihewan Basin directly dated by magnetostratigraphy. Data sources for the faunas: HY (Huang and Tang, 1974); XSG (Teilhard de Chardin and Piveteau, 1930; Zhou et al., 1991); HBG-II (Wang, 1982); HBG-I (Wang, 1982; Zhou et al., 1991); YSZ (Ao et al., 2013); MJG-III (Zhu et al., 2004); XCL (You et al., 1980; Tang et al., 1995); BS (Wei, 1994); DGT (Wei et al., 1985; Wei, 1991); ML (Wei, 1991); XJY (Jia and Wei, 1976; Jia et al., 1979).

Taxa	Faunas											
	HY (2.4 Ma)	XSG (1.7–2.2 Ma)	HBG-II (1.9 Ma)	HBG-I (1.7 Ma)	YSZ-II (1.8 Ma)	YSZ-I (1.6 Ma)	MJG-III (1.66 Ma)	XCL (1.36 Ma)	BS (1.32 Ma)	DGT (1.1 Ma)	ML (0.8 Ma)	XJY (0.5 Ma)
Acinonyx sp.						+						
Allactaga cf. *annulatus*		+										
Allophaiomys. cf. *A. pliocaenicus*								+				
Antilospiroides hobeiensis				+								
Bison sp.		+								+		
Bovinae indet.								+				
Bos primigenius												+
Canis sp.			+				+			+		
Canis chihliensis		+										
Canis multicuspus			+									
Canis lupus												+
Carnivora gen. et sp. indet.							+					
Cervulus cf. *sinensis*		+										
Cervus sp.		+					+	+				+
Chilotherium sp.	+											
Circotherium sp.		+										
Coelodonta antiquitatis		+					+	+	+	+	+	+
Cynailurus pleistocaenicus		+										
Elaphurus bifurcatus		+										
Elasmotherium peii		+										
Elephas sp.		+					+					
Equus przewalski												+
Equus huanghoensis						+						
Equus sanmeniensis		+			+		+	+		+		
Equus sp.									+		+	
Erinaceus cf. *dealbatus*		+										
Eucladoceros		+										
Felis sp.		+										
Gazella sp.			+	+			+	+		+		+
Gazella blacki			+	+								
Gazella sinensis		+										
Gazella subgutturosa		+										+
Hipparion sp.	+		+					+				
Hipparion houfenense				+								
Hipparion cf. *hippidiodus*			+									
Hyaena sp.		+										
Hyaena licenti		+										
Leporidae gen. et sp. indet.			+									
Lutra licenti		+										
Lynx shansius		+										
Martes sp.								+				
Machairodus nihowanensis		+										
Megaloceros ordosianus												+
Meles cf. *leucurus*		+										
Microtus brandtioides												+
Mimomys chinensis								+				
Mimomys orientalis												+
Mustela pachygnathus		+										
Myospalax tingi		+										
Myospalax cf. *fontanieri*										+		+
Nyctereutes sinensis		+	+									
Nyctereutes sp.						+						
Ochotona sp.												+
Ochotona lagrelii		+										
Ochotona complicidens		+										
Orientalomys nihowanicus		+										
Ovis shantungensis		+										
Pachycrocuta licenti								+				
Pachycrocuta sp.							+					
Palaeoloxodon sp.		+						+		+	+	+
Palaeoloxodon namadicus		+										
Palaeotragus sp.			+									
Panthera cf. *tigris*												+
Paracamelus gigas		+										
Pliohyrax sp.		+										
Postschizotherium sp.				+								
Proboscidipparion sinensis		+						+				
Procapra picticaudata przewalski												+
Prosiphneus sp.												
Rhinoceros sinensis		+										

Table 2 (*continued*)

Taxa	Faunas											
	HY (2.4 Ma)	XSG (1.7–2.2 Ma)	HBG-II (1.9 Ma)	HBG-I (1.7 Ma)	YSZ-II (1.8 Ma)	YSZ-I (1.6 Ma)	MJG-III (1.66 Ma)	XCL (1.36 Ma)	BS (1.32 Ma)	DGT (1.1 Ma)	ML (0.8 Ma)	XJY (0.5 Ma)
Rusa elegans		+										
Sinoryx sp.				+								
Spirocerus		+										+
Struthio sp.							+					+
Sus cf. *lydekkeri*		+										
Sus sp.												+
Ursus cf. *etruscus*		+										
Viverra sp.				+								
Vulpes sp.		+										

This decreased chemical weathering intensity is linked to a long-term increase in cooling and aridification (Ao et al., 2009, 2010b).

Investigations of mammalian fossils indicate that the taxonomic composition and faunal properties of the mammals are sensitive to environmental changes (e.g., Tougard and Montuire, 2006; Kuzmina et al., 2011; Matthews et al., 2011; Li et al., 2012), thus fossil mammals can provide various clues to achieve a better understanding of the general setting of early human evolution during the Pleistocene. Generally, the Nihewan Fauna contains both typical grassland (e.g., horses, gazelles, hares, camels, jerboas, gerbils, hamsters, hyenas) and woodland (e.g., tigers, bears, Eurasian pigs, lynxes, badgers, apodemuses, harvest mice, elephants) species (Tables 1–3). So, mixed grassland and woodland habitats were prevalent at the time that early humans occupied the basin during the Pleistocene. For these well-dated faunas, we further calculated the occurrence of woodland and grassland mammalian groups as percentages (Fig. 11). Fossil mammals referred to as woodland species include tigers, bears, Eurasian pigs, lynxes, badgers, apodemuses, harvest mice and elephants. The fossil mammals referred to grassland species include horses, gazelles, hares, camels, jerboas, gerbils, hamsters, hyenas. Other mammals such as wolves, foxes, cats and giraffes have equal adaptability to forests and grasslands, which makes it difficult to estimate the specific environment in which they lived.

All faunas appear to be dominated by grassland species (≥50%), except for the YSZ-I and XSG faunas (Fig. 11). The BS, DD-1, YSZ-II and HY faunas are characterized by grassland species only, but the relatively small number of mammal species may have resulted in an overestimation of the grassland cover (Fig. 11). Mineral magnetic properties, clay mineralogy and geochemistry of the Nihewan Formation at the Xiantai (XT) section indicate a long-term aridification and cooling trend of the regional Nihewan Basin (Ao et al., 2009, 2010b; Ao, 2010) (Fig. 10c–f). This is consistent with the global cooling suggested by the marine isotope oxygen record (Lisiecki and Raymo, 2005) (Fig. 10g) and development of Asian aridification and cooling indicated by mineral magnetism of Chinese loess (Deng et al., 2006a). However, the Nihewan Fauna is not indicative of either a long-term increasing trend in grassland species or a long-term decreasing trend in woodland species (Fig. 11), which seems to be inconsistent with the inferred long-term climate variability in the Nihewan Basin. This apparent inconsistency may be due to a lower sampling resolution of the faunas. Alternatively, it is also possible that the mammals and vegetation might be less sensitive to this long-term climate variability. As suggested by Fig. 10g, this long-term climate variability is generally associated with glacial–interglacial cycles. The low sampling resolution of the faunas could mean that these climate variations are not evident in the relative percentages of grassland and woodland mammalian species (Fig. 11). At present, the Nihewan Basin has become less suitable for forest and even grass cover because of the disappearance of lake and enhanced aridity. However, the Xujiayao Fauna indicates that some forests still existed around the Nihewan paleolake and surrounding mountains at least 0.5 Myr ago (Fig. 11).

5.4. Implications for early human occupation in the Nihewan Basin

During the Pleistocene, the Nihewan Basin was one of the most important cradles of early human evolution in East Asia after initial hominin migration out of Africa (Schick and Dong, 1993; Gao et al., 2005; Dennell, 2009; Keates, 2010). Most of the Lower Paleolithic sites that have been found in China are from the Nihewan Basin, such as the magnetostratigraphically dated MJG (1.66–1.55 Ma) (Zhu et al., 2004), Lanpo (LP) (~1.6 Ma) (Ao et al., 2012), XCL (1.36 Ma) (Zhu et al., 2001), XT (1.36 Ma) (Deng et al., 2006b), BS (1.32 Ma) (Zhu et al., 2004), Feiliang (FL) (1.2 Ma) (Deng et al., 2007; Ao et al., 2012), Cenjiawan (CJW) (1.1 Ma) (Wang et al., 2006), DGT (1.1 Ma) (Wang et al., 2005), Huojiadi (HJD) (1.0 Ma) (Liu et al., 2010a), ML (0.78 Ma) (Wang et al., 2005), XJY (0.5 Ma) (Løvlie et al., 2001; Wang et al., 2008) and Hougou (HG) (0.4 Ma) (Zuo et al., 2011) Paleolithic sites. Combining the electron spin resonance (ESR) dating of the Dongpo (DP) site (~0.3 Ma) (Liu et al., 2010c), we have established a magnetochronological framework for the Paleolithic sites in this basin, which ranges from ca 1.7 to 0.3 Ma (Fig. 10b). Although early humans encountered climatic and environmental variability of global and regional significance, such as the regionally decreased winter temperature and long-term increase in aridity and cooling, they still flourished in the Nihewan Basin during most of the Pleistocene (Fig. 10). It seems that early humans were able to use widely different animal and plant resources under a variety of high-latitude climatic regimes in North China during the Early Pleistocene, which indicates a high level of adaptability. Natural selection pressures posed by large-scale climate variability possibly further promoted the evolution of early humans outside of Africa and enhanced their ability in certain ways (deMenocal, 2011). The general coexistence of Paleolithic and faunal sites (Fig. 10b) implies that early humans in the Nihewan Basin preyed on and ate large grazing animals. For example, diaphysis fragments of deer- and horse-sized mammalian long bones at the MJG-III Paleolithic site contain clear tool percussion damage indicative of marrow extraction, which represents the oldest (1.66 Ma) known use of animal tissues for food (Zhu et al., 2004). Hunting and eating of animals are suggested to have been crucial for living in the cold climate of the Nihewan Basin, such as the overwintering problem of the 40°N temperate zone (Zhu et al., 2004; Deng et al., 2007; Ao et al., 2010b). In addition to a substantial body of water and abundant large mammals as food sources, the presence of mixed savannah and woodland habitats like in Africa may be another major attractor for early human colonization of the Nihewan Basin during the Early Pleistocene. Together with the

Table 3
Mammal list of the Danangou (DNG) (Li, 1984), Dongyaozhitou (DYZT) (Tang, 1980; Zhou et al., 1991) and Xinyaozi (XYZ) (Zhou et al., 1991) faunas in the northeastern Nihewan Basin.

Taxa	Faunas		
	XYZ	DYZT	DNG
Struthis cf. *anderossioni*	+		
Erinaceus cf. *dealbatus*	+		
Lepus cf. *wongi*	+		
Ochotona complicidens	+		
Mimomys chinensis	+		
Myospalax omegodon	+		
Cricetulus varians	+		
Nyctereutes sinensis	+	+	
Canis chihliensis	+		+
Meles chiai	+		+
Agriontherium sp.	+		
Hyaena licenti	+		
Megantereon nihowanensis	+		
Homotherium cf. crenatiders	+		
Lynx shansius	+		
Felis peii	+		
Postschizotheriums intermedium	+		
Palaeoloxodon namadicus	+		
Proboscidipparion sinense	+	+	
Equus sanmeniensis	+		+
Dicerorhinus mercki	+		
Elasmotherium sp.	+		
Sus cf. *lydekkeri*	+		
Muntiacus sinensis	+		
Elaphurus bifurcatus	+		
Eucladoceros boulei	+		
Cervus (Rusa) elegans	+		
Gazella sinensis	+	+	+
Gazella cf. *subgutturosa*	+		
Spirocerus wongi	+		
Antilospira robusta	+		
Protoryx sp.	+		
Coelodonta antiquitatis		+	+
Lynx variabilis		+	
Dipoides sp.		+	
Zygolophodon sp.		+	
Hipparion houfenense		+	
Axis sp.		+	
Antilospira yuxianensis		+	
Palaeotragus progressvus		+	
Paracamelus sp.		+	
Ochotona lagrelii			+
Orientalomys nihowanicus			+
Hyaena sp.			+
Proboscidipparion sinensis			+
Vulpes sp.			+

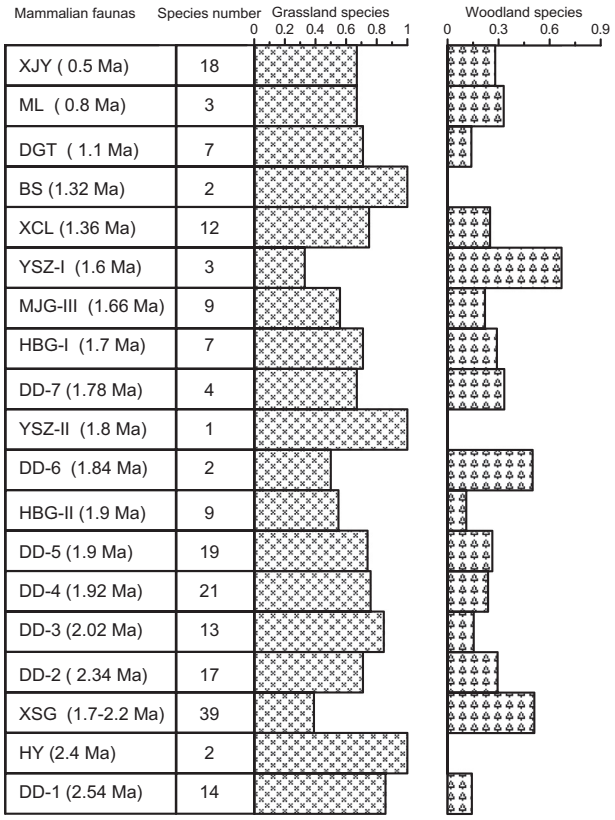

Fig. 11. Variability of the total number of mammalian species and percentages of grassland and woodland groups for the well-dated Pleistocene faunas in the Nihewan Basin.

Paleolithic sites of Xihoudu dated at 1.27 Ma (Zhu et al., 2003) and Gongwangling at 1.15 Ma (An and Ho, 1989) on the southern margin of the Chinese Loess Plateau (see Fig. 1 for locations), eleven >1 Ma Paleolithic sites have been documented in North China. Unlike North China, the lush and densely vegetated low-latitude East Asia has rare evidence of hominins before 1 Ma, although it had a much warmer climate than North China. Currently such hominin evidence from low-latitude East Asia comes mainly from the Yuanmou Basin (ca 1.7 Ma) in South China (Zhu et al., 2008) and Java (1.51 Ma) in southeast Asia (Larick et al., 2001). The warm and humid subtropical climate generally results in lush primal forests in South China inhabited by the *Ailuropodae-Stegodon* fauna, which included the giant panda, gibbons, orangutans and the giant extinct ape *Gigantopithecus* (Wang et al., 2007; Rink et al., 2008; Jin et al., 2009). The forests and faunas may have formed a less attractive ecology for the savanna-adapted early humans in South China. This may be one of the reasons why North China has much more evidence of Early Pleistocene humans than South China.

The stone artifacts in the Nihewan Basin are technologically simple, characterized by apparently uneconomical use of stone, generally informal artifacts and rare occurrence of retouched flake and core platforms (Keates, 2000, 2010; Shen, 2007; Dennell, 2009; Liu et al., 2013). Tool assemblages are dominated by irregular cores, flakes and scrapers. Direct hammer percussion is the main method used for flake knapping. The irregular shape of most cores and flakes implies that the lithic technology was highly expedient, with little foresight beyond the production of the next flake. Raw materials for the stone tools are generally low quality flints acquired near the sites. This lithic technology is similar to the Oldowan technique (sensu stricto) in Africa. In the Nihewan Basin, it lasted for over one million years, from the earliest sites such as MJG (1.66–1.55 Ma) (Zhu et al., 2004) and LP (1.6 Ma) (Ao et al., 2012) to the later sites such as BS (1.32 Ma) (Zhu et al., 2004), DGT (1.1 Ma) and ML (0.78 Ma) (Wang et al., 2005), and further to the latest sites such as Hougou (HG) (0.4 Ma) (Zuo et al., 2011) and Dongpo (DP) (~0.3 Ma) (Liu et al., 2010c). Up to now, the more advanced Acheulean technology characterized by shaped bifacial stone tools (Isaac and Curtis, 1974; de la Torre, 2011; Lepre et al., 2011) has not been found in the Nihewan Basin (Xie, 2006; Xie et al., 2006; Yuan et al., 2011). Also it was absent in the Xihoudu (Zhu et al., 2003) and Gongwangling sites (An and Ho, 1989). However, it emerged in the Bose Basin in South China as early as 0.8 Ma (Hou et al., 2000). This indicates that multiple groups of hominins distinguished by separate stone-tool-making behavior may have coexisted in China after 0.8 Ma. A similar coexistence of Acheulean and Oldowan artifacts has been found in Africa and India as early as 1.76 and 1.1–1.5 Ma, respectively (Lepre et al., 2011; Pappu et al., 2011). This also suggests that some hominins were able to survive in North China for

most of the Pleistocene (ca 1.7–0.3 Ma) using a simple Oldowan-like technique.

6. Conclusions

(1) Magnetostratigraphic results indicate that the DD fluvio-lacustrine section in the eastern Nihewan Basin records the lowermost Brunhes normal polarity chron, the Matuyama reversed polarity chron and the late Gauss normal polarity chron. The Jaramillo and Olduvai normal polarity subchrons in the Matuyama chron are also identified.
(2) Seven mammalian fossil-bearing layers of the Daodi Fauna are shown to be located between the Gauss–Matuyama boundary and the termination of the Olduvai polarity subchron, which are estimated to have a time range of ca 2.5–1.8 Ma.
(3) Combining our new and previously published magnetostratigraphic data, we establish a Pleistocene chronological framework of ca 2.4–0.5 Ma for the faunas and ca 1.7–0.3 Ma for the Paleolithic sites in the Nihewan Basin.
(4) Occurrence of both woodland and grassland mammalian groups in the Nihewan Fauna indicates mixed savannah and woodland habitats for early humans in the Nihewan Basin similar to these in Africa during the Pleistocene.
(5) The Nihewan hominins consistently adopted a simple Oldowan-like technology from at least ca 1.7 to 0.3 Ma. A more advanced Acheulean technology has not been found in the Nihewan Basin, although it started to emerge in the Bose Basin of South China at ca 0.8 Ma. This implies that multiple groups of hominins distinguished by differential stone-tool-making capabilities may have coexisted in China after 0.8 Ma.

Acknowledgments

We thank the anonymous reviewers for their insightful comments, which were helpful in improving this paper. This study was financially supported by the National Natural Science Foundation of China (41174057), the Key Projects of National Basic Research Program of China (2010CB833400), and the West Light Foundation of the Chinese Academy of Sciences.

Editorial handling by: R. Grun

Appendix A. Supplementary data

Supplementary data related to this article can be found at http://dx.doi.org/10.1016/j.quageo.2013.06.004.

References

An, Z.S., Ho, C.K., 1989. New magnetostratigraphic dates of Lantian *Homo erectus*. Quaternary Research 32, 213–221.
Ao, H., 2008. Rock magnetic properties of the fluvio-lacustrine sediments from the Dachangliang section in the Nihewan Basin, northern China. Chinese Journal of Geophysics 51, 1029–1039 (in Chinese with English abstract).
Ao, H., 2010. Mineral-magnetic signal of long-term climatic variation in Pleistocene fluvio-lacustrine sediments, Nihewan Basin (North China). Journal of Asian Earth Sciences 39, 692–700.
Ao, H., Dekkers, M.J., Deng, C.L., Zhu, R.X., 2009. Paleoclimatic significance of the Xiantai fluvio-lacustrine sequence in the Nihewan Basin (North China), based on rock magnetic properties and clay mineralogy. Geophysical Journal International 177, 913–924.
Ao, H., Deng, C.L., Dekkers, M.J., Liu, Q.S., 2010a. Magnetic mineral dissolution in Pleistocene fluvio-lacustrine sediments, Nihewan Basin (North China). Earth and Planetary Science Letters 292, 191–200.
Ao, H., Deng, C.L., Dekkers, M.J., Sun, Y.B., Liu, Q.S., Zhu, R.X., 2010b. Pleistocene environmental evolution in the Nihewan Basin and implication for early human colonization of North China. Quaternary International 223–224, 472–478.
Ao, H., An, Z.S., Dekkers, M.J., Wei, Q., Pei, S.W., Zhao, H., Zhao, H.L., Xiao, G.Q., Qiang, X.K., Wu, D.C., Chang, H., 2012. High-resolution record of geomagnetic excursions in the Matuyama chron constrains the ages of the Feiliang and Lanpo Paleolithic sites in the Nihewan Basin, North China. Geochemistry, Geophysics, Geosystems 13, Q08017. http://dx.doi.org/10.1029/2012GC004095.
Ao, H., Dekkers, M.J., An, Z.S., Xiao, G.Q., Li, Y.X., Zhao, H., Qiang, X.K., Chang, H., Zhao, H., Chang, Q.H., Wu, D.C., 2013. Magnetostratigraphic evidence of a mid-Pliocene onset of the Nihewan Formation – implications for early fauna and hominid occupations in the Nihewan Basin, North China. Quaternary Science Reviews 59, 30–42.
Barbour, G.B., 1924. Preliminary observation in Kalgan Area. Bulletin of Geological Society of China 3, 167–168.
Beden, M., 1980. *Elephas recki* Dietrich, 1915 (Proboscidea, Elephantidae). Evolution au cours du Plio-Pleistocene en Afrique orientale. Geobios 13, 891–901.
Cai, B.Q., 1987. A preliminary report on the late Pliocene micromammalian fauna from Yangyuan and Yuxian, Hebei. Vertebrata Palasiatica 25, 124–136 (in Chinese with English abstract).
Cai, B.Q., Zhang, Z.Q., Zheng, S.H., Qiu, Z.D., Li, Q., 2004. New advances in the stratigraphic study on representative sections in the Nihewan Basin, Heibei. Professional Papers on Stratigraphy and Paleontology 28, 267–285 (in Chinese with English abstract).
de la Torre, I., 2011. The early stone age lithic assemblages of Gadeb (Ethiopia) and the developed Oldowan/early Acheulean in East Africa. Journal of Human Evolution 60, 768–812.
deMenocal, P.B., 2011. Climate and human evolution. Science 331, 540–542.
Deng, C.L., Shaw, J., Liu, Q.S., Pan, Y.X., Zhu, R.X., 2006a. Mineral magnetic variation of the Jingbian loess/paleosol sequence in the northern Loess Plateau of China: implications for Quaternary development of Asian aridification and cooling. Earth and Planetary Science Letters 241, 248–259.
Deng, C.L., Zhu, R.X., Zhang, R., Ao, H., Pan, Y.X., 2008. Timing of the Nihewan formation and faunas. Quaternary Research 69, 77–90.
Deng, C.L., Xie, F., Liu, C.C., Ao, H., Pan, Y.X., Zhu, R.X., 2007. Magnetochronology of the Feiliang Paleolithic site in the Nihewan Basin and implications for early human adaptability to high northern latitudes in East Asia. Geophysical Research Letters 34, L14301. doi: 14310.11029/12007GL030335.
Deng, C.L., Wei, Q., Zhu, R.X., Wang, H.Q., Zhang, R., Ao, H., Chang, L., Pan, Y.X., 2006b. Magnetostratigraphic age of the Xiantai Paleolithic site in the Nihewan Basin and implications for early human colonization of Northeast Asia. Earth and Planetary Science Letters 244, 336–348.
Deng, T., Xue, X.X., 1999. Chinese Fossil Horses of *Equus* and their Environment. China Ocean Press, Beijing (in Chinese with English abstract).
Deng, T., Wang, X.M., Fortelius, M., Li, Q., Wang, Y., Tseng, Z.J.J., Takeuchi, G.T., Saylor, J.E., Saila, L.K., Xie, G.P., 2011. Out of Tibet: Pliocene woolly rhino suggests high-plateau origin of Ice Age megaherbivores. Science 333, 1285–1288.
Dennell, R.W., 2009. The Palaeolithic Settlement of Asia. Cambridge University Press, Cambridge.
Dunlop, D.J., Özdemir, Ö., 1997. Rock Magnetism: Fundamentals and Frontiers. Cambridge University Press, Cambridge.
Flynn, L.J., Wu, W., Downs, W.R., 1997. Dating vertebrate microfaunas in the late Neogene record of Northern China. Palaeogeography, Palaeoclimatology, Palaeoecology 133, 227–242.
Gao, X., Wei, Q., Shen, C., Keates, S.G., 2005. New light on the earliest hominid occupation in East Asia. Current Anthropology 46, 115–120.
Gibbard, P.L., Head, M.J., 2010. The newly-ratified definition of the Quaternary System/Period and redefinition of the Pleistocene Series/Epoch, and comparison of proposals advanced prior to formal ratification. Episodes 33, 152–158.
Hilgen, F.J., Lourens, L.J., van Dam, J.A., 2012. The Neogene Period. In: Gradstein, F.M., Ogg, J.G., Schmitz, M., Ogg, G. (Eds.), The Geologic Time Scale. Elsevier, Amsterdam, pp. 923–978.
Hou, Y.M., Potts, R., Yuan, B.Y., Guo, Z.T., Deino, A., Wang, W., Clark, J., Xie, G.M., Huang, W.W., 2000. Mid-Pleistocene Acheulean-like stone technology of the Bose basin, South China. Science 287, 1622–1626.
Huang, W.P., Tang, Y.J., 1974. Observation on the later Cenozoic of Nihewan Basin. Vertebrata Palasiatica 12, 99–110 (in Chinese with English abstract).
Isaac, G.L., Curtis, G.H., 1974. Age of early Acheulian industries from the Peninj Group, Tanzania. Nature 249, 624–627.
Jia, L.P., Wei, Q., Li, C.R., 1979. Report on the excavation of Hsuchiayao Man Site in 1976. Vertebrata Palasiatica 17, 277–293 (in Chinese with English abstract).
Jia, L.P., Wei, Q., 1976. Xujiayao Palaeolithic site, in Yanggao County, Shanxi Province. Archaeology Bulletin 2, 97–114 (in Chinese).
Jin, C.Z., Qin, D.G., Pan, W.S., Tang, Z.L., Liu, J.Y., Wang, Y., Deng, C.L., Zhang, Y.Q., Dong, W., Tong, H.W., 2009. A newly discovered Gigantopithecus fauna from Sanhe Cave, Chongzuo, Guangxi, South China. Chinese Science Bulletin 54, 788–797.
Jones, C.H., 2002. User-driven integrated software lives: "Paleomag" paleomagnetics analysis on the Macintosh. Computers and Geosciences 28, 1145–1151.
Keates, S.G., 2000. Early and middle pleistocene hominid behaviour in Northern China. British Archaeological Reports 863, 1–387.
Keates, S.G., 2010. Evidence for the earliest Pleistocene hominid activity in the Nihewan Basin of northern China. Quaternary International 223, 408–417.
Kirschvink, J.L., 1980. The least-squares line and plane and the analysis of paleomagnetic data. Geophysical Journal of the Royal Astronomical Society 62, 699–718.
Kuzmina, S.A., Sher, A.V., Edwards, M.E., Haile, J., Yan, E.V., Kotov, A.V., Willerslev, E., 2011. The late Pleistocene environment of the Eastern West Beringia based on the principal section at the Main River, Chukotka. Quaternary Science Reviews 30, 2091–2106.
Larick, R., Ciochon, R.L., Zaim, Y., Suminto, S., Rizal, Y., Aziz, F., Reagan, M., Heizler, M., 2001. Early Pleistocene $^{40}Ar/^{39}Ar$ ages for Bapang Formation hom-

inins, Central Jawa, Indonesia. Proceedings of the National Academy of Sciences of the United States of America 98, 4866–4871.
Lepre, C.J., Roche, H., Kent, D.V., Harmand, S., Quinn, R.L., Brugal, J.P., Texier, P.J., Lenoble, A., Feibel, C.S., 2011. An earlier origin for the Acheulian. Nature 477, 82–85.
Li, Q., Zheng, S.H., Cai, B.Q., 2008. Pliocene biostratigraphic sequence in the Nihewan Basin, Hebei, China. Vertebrata Palasiatica 46, 210–232 (in Chinese with English abstract).
Li, Y., 1984. The early Pleistocene mammalian fossils of Danangou, Yuxian, Hebei. Vertebrata Palasiatica 22, 60–68 (in Chinese with English abstract).
Li, Y.X., Zhang, Y.X., Xue, X.X., 2012. The composition of three mammal faunas and environmental evolution in the last glacial maximum, Guanzhong area, Shaanxi Province, China. Quaternary International 248, 86–91.
Lindsay, E.H., Opdyke, N.D., Johnson, N.M., 1980. Pliocene dispersal of the horse *Equus* and late Cenozoic mammalian dispersal events. Nature 287, 135–138.
Lisiecki, L.E., Raymo, M.E., 2005. A Pliocene–Pleistocene stack of 57 globally distributed benthic $\delta^{18}O$ records. Paleoceanography 20, PA1003. http://dx.doi.org/1010.1029/2004PA001071.
Liu, P., Deng, C.L., Li, S.H., Zhu, R.X., 2010a. Magnetostratigraphic dating of the Huojiadi Paleolithic site in the Nihewan Basin, North China. Palaeogeography, Palaeoclimatology, Palaeoecology 298, 399–408.
Liu, P., Deng, C.L., Li, S.H., Cai, S.H., Cheng, H.J., Yuan, B.Y., Wei, Q., Zhu, R.X., 2012. Magnetostratigraphic dating of the Xiashagou Fauna and implication for sequencing the mammalian faunas in the Nihewan Basin, North China. Palaeogeography, Palaeoclimatology, Palaeoecology 315–316, 75–85.
Liu, Q.S., Deng, C.L., Yu, Y.J., Torrent, J., Jackson, M.J., Banerjee, S.K., Zhu, R.X., 2005. Temperature dependence of magnetic susceptibility in an argon environment: implications for pedogenesis of Chinese loess/palaeosols. Geophysical Journal International 161, 102–112.
Liu, Q.S., Torrent, J., Morrás, H., Ao, H., Jiang, Z.X., Su, Y.L., 2010b. Superparamagnetism of two modern soils from the northeastern Pampean region, Argentina and its paleoclimatic indications. Geophysical Journal International 183, 695–705.
Liu, C.R., Yin, G.M., Gao, L., Bahain, J.J., Li, J.P., Lin, M., Chen, S.M., 2010c. ESR dating of Pleistocene archaeological localities of the Nihewan Basin, North China – preliminary results. Quaternary Geochronology 5, 385–390.
Liu, Y., Hu, Y.Q., Wei, Q., 2013. Early to Late Pleistocene human settlements and the evolution of lithic technology in the Nihewan Basin, North China: a macroscopic perspective. Quaternary International 295, 204–214.
Løvlie, R., Su, P., Fan, X.Z., Zhao, Z.J., Liu, C., 2001. A revised paleomagnetic age of the Nihewan Group at the Xujiayao Palaeolithic Site, China. Quaternary Science Reviews 20, 1341–1353.
Matthews, T., Rector, A., Jacobs, Z., Herries, A.I.R., Marean, C.W., 2011. Environmental implications of micromammals accumulated close to the MIS 6 to MIS 5 transition at Pinnacle Point Cave 9 (Mossel Bay, Western Cape Province, South Africa). Palaeogeography, Palaeoclimatology, Palaeoecology 302, 213–229.
May, S.R., Butler, R.F., 1986. North American Jurassic apparent polar wander: implications for plate motion, paleogeography and Cordilleran Tectonics. Journal of Geophysical Research 91, 1519–1544.
McFadden, P.L., McElhinny, M.W., 1990. Classification of the reversal test in paleomagnetism. Geophysical Journal International 103, 725–729.
Pappu, S., Gunnell, Y., Akhilesh, K., Braucher, R., Taieb, M., Demory, F., Thouveny, N., 2011. Early Pleistocene presence of Acheulian hominins in South India. Science 331, 1596–1599.
Qiu, Z.X., 2000. Nihewan fauna and Q/N boundary in China. Quaternary Science 20, 142–154 (in Chinese with English abstract).
Rees, A.I., Wooddall, W.A., 1975. The magnetic fabric of some laboratory deposited sediments. Earth and Planetary Science Letters 25, 121–130.
Rink, W.J., Wei, W., Bekken, D., Jones, H.L., 2008. Geochronology of Ailuropoda-Stegodon fauna and Gigantopithecus in Guangxi Province, southern China. Quaternary Research 69, 377–387.
Schick, K.D., Dong, Z., 1993. Early paleolithic of China and eastern Asia. Evolutionary Anthropology 2, 22–35.
Shen, C., 2007. Lithic technology and hominid behaviour of the earliest occupations at the Nihewan Basin, northern China. American Journal of Physical Anthropology, 216.
Tang, Y.J., 1980. Note on a small collection of early Pleistocene mammalian fossils from northern Hebei. Vertebrata Palasiatica 18, 314–323 (in Chinese with English abstract).
Tang, Y.J., Li, Y., Chen, W.Y., 1995. Mammalian fossils and the age of Xiaochangliang paleolithic site of Yangyuan, Hebei. Vertebrata Palasiatica 33, 74–83 (in Chinese with English abstract).
Tanikawa, W., Mishima, T., Hirono, T., Soh, W., Song, S.R., 2008. High magnetic susceptibility produced by thermal decomposition of core samples from the Chelungpu fault in Taiwan. Earth and Planetary Science Letters 272, 372–381.
Tauxe, L., 1998. Paleomagnetic Principles and Practice. Kluwer Academic Publishers, Dordrecht.
Tchernov, E., Shoshani, J., 1996. Proboscidean remains in southern Levant. In: Shoshani, J., Tassy, P. (Eds.), The Proboscidea. Oxford University Press, Oxford, pp. 225–233.
Teilhard de Chardin, P., Piveteau, J., 1930. Les mammiferes fossils de Nihowan (Chine). Annales de Paleontologie 19, 1–154.
Tougard, C., Montuire, S., 2006. Pleistocene paleoenvironmental reconstructions and mammalian evolution in South-East Asia: focus on fossil faunas from Thailand. Quaternary Science Reviews 25, 126–141.
van Velzen, A.J., Zijderveld, J.D.A., 1995. Effects of weathering on single-domain magnetite in Early Pliocene marine marls. Geophysical Journal International 121, 267–278.
Wang, A.D., 1982. Discovery of the Pliocene mammalian faunas from the Nihewan region and its significance. Chinese Science Bulletin 27, 227–229.
Wang, H.Q., Deng, C.L., Zhu, R.X., Xie, F., 2006. Paleomagnetic dating of the Cenjiawan Paleolithic site in the Nihewan Basin, northern China. Science in China 49, 295–303.
Wang, H.Q., Deng, C.L., Zhu, R.X., Wei, Q., Hou, Y.M., Boeda, E., 2005. Magnetostratigraphic dating of the Donggutuo and Maliang Paleolithic sites in the Nihewan Basin, North China. Quaternary Research 64, 1–11.
Wang, S.Q., Deng, T., 2011. Some evolutionary trends of *Equus eisenmannae* (Mammalia, Perissodactyla) in the stratigraphic sequence of Longdan, China, in comparison to modern *Equus*. Journal of Vertebrate Paleontology 31, 1356–1365.
Wang, W., Potts, R., Baoyin, Y., Huang, W.W., Cheng, H., Edwards, R.L., Ditchfield, P., 2007. Sequence of mammalian fossils, including hominoid teeth, from the Bubing Basin caves, South China. Journal of Human Evolution 52, 370–379.
Wang, X.S., Yang, Z.Y., Løvlie, R., Min, L.R., 2004. High-resolution magnetic stratigraphy of fluvio-lacustrine succession in the Nihewan Basin, China. Quaternary Science Reviews 23, 1187–1198.
Wang, X.S., Løvlie, R., Su, P., Fan, X.Z., 2008. Magnetic signature of environmental change reflected by Pleistocene lacustrine sediments from the Nihewan Basin, North China. Palaeogeography, Palaeoclimatology, Palaeoecology 260, 452–462.
Wei, Q., 1991. Geologic sequence of the archaeological sites in the Nihewan Basin, North China. In: IVPP (Institute of Vertebrate Paleontology and Paleoanthropology) (Ed.), Contributions to the XIII INQUA. Beijing Scientific and Technological Publishing House, Beijing, pp. 61–73 (in Chinese).
Wei, Q., 1994. Banshan Paleolithic site from the Lower Pleistocene in the Nihewan Basin in northern China. Acta Anthropologica Sinica 13, 223–238 (in Chinese).
Wei, Q., Meng, H., Cheng, S.Q., 1985. New Paleolithic site from the Nihewan beds. Acta Anthropologica Sinica 4, 223–232 (in Chinese).
Xie, F., 2006. Nihewan. Cultural Relics Publishing House, Beijing (in Chinese).
Xie, F., Li, J., Liu, L.Q., 2006. Paleolithic Archeology in the Nihewan Basin. Huashan Literature & Arts Press, Shijiazhuang (China) (in Chinese).
You, Y.Z., Tang, Y.J., Li, Y., 1980. Discovery of the Palaeolithics from the Nihewan Formation. Quaternary Science 5, 1–11 (in Chinese).
Young, C.C., 1950. The Plio-Pleistocene boundary in China. In: Report on 18th International Geological Congress, London, pp. 115–125.
Yuan, B.Y., Xia, Z.K., Niu, P.S., 2011. Nihewan Rift and Early Man. China Geological Press, Beijing (in Chinese).
Zhang, C.X., Paterson, G.A., Liu, Q.S., 2012. A new magnetic enhancement mechanism of hematite during heating: the role of clay minerals. Studia Geophysica et Geodaetica 56, 845–860.
Zhang, C.X., Liu, Q.S., Huang, B.C., Su, Y.L., 2010. Magnetic enhancement upon heating of environmentally polluted samples containing haematite and iron. Geophysical Journal International 181, 1381–1394.
Zhang, Z.Q., Zheng, S.H., Liu, J.B., 2003. Pliocene micromammalian biostratigraphy of Nihewan Basin, with comments on the stratigraphic division. Vertebrata Palasiatica 41, 306–313 (in Chinese with English abstract).
Zheng, S.H., Zhang, Z.Q., 2001. Late Miocene–Early Pleistocene biostratigraphy of the Leijiahe area, Lingtai, Gansu. Vertebrata Palasiatica 39, 215–228 (in Chinese with English abstract).
Zhou, T.R., Li, H.Z., Liu, Q.S., Li, R.Q., Sun, X.P., 1991. Cenozoic Paleogeography of the Nihewan Basin. China Science Press, Beijing (in Chinese).
Zhu, R.X., Deng, C.L., Pan, Y.X., 2007. Magnetochronology of the fluvio-lacustrine sequences in the Nihewan basin and its implications for early human colonization of Northeast Asia. Quaternary Science 27, 922–944 (in Chinese with English abstract).
Zhu, R.X., An, Z.S., Potts, R., Hoffman, K.A., 2003. Magnetostratigraphic dating of early humans in China. Earth-Science Reviews 61, 341–359.
Zhu, R.X., Potts, R., Pan, Y.X., Yao, H.T., Lu, L.Q., Zhao, X., Gao, X., Chen, L.W., Gao, F., Deng, C.L., 2008. Early evidence of the genus Homo in East Asia. Journal of Human Evolution 55, 1075–1085.
Zhu, R.X., Hoffman, K.A., Potts, R., Deng, C.L., Pan, Y.X., Guo, B., Shi, C.D., Guo, Z.T., Yuan, B.Y., Hou, Y.M., Huang, W.W., 2001. Earliest presence of humans in northeast Asia. Nature 413, 413–417.
Zhu, R.X., Potts, R., Xie, F., Hoffman, K.A., Deng, C.L., Shi, C.D., Pan, Y.X., Wang, H.Q., Shi, R.P., Wang, Y.C., Shi, G.H., Wu, N.Q., 2004. New evidence on the earliest human presence at high northern latitudes in northeast Asia. Nature 431, 559–562.
Zijderveld, J.D.A., 1967. AC demagnetization of rocks: analysis of results. In: Collinson, D.W., Creer, K.M., Runcorn, S.K. (Eds.), Methods in Paleomagnetism. Elsevier, New York, pp. 254–286.
Zuo, T.W., Cheng, H.J., Liu, P., Xie, F., Deng, C.L., 2011. Magnetostratigraphic dating of the Hougou Paleolithic site in the Nihewan Basin, North China. Science in China 54, 1643–1650.